Interfacial Properties of LiTFSI and LiPF6-Based Electrolytes in Binary and Ternary Mixtures of Alkylcarbonates on Graphite Electrodes and Celgard Separator

Published in:
Industrial and Engineering Chemistry Research

Interfacial Properties of LiTFSI and LiPF$_6$-Based Electrolytes in Binary and Ternary Mixtures of Alkylcarbonates on Graphite Electrodes and Celgard Separator

Mouad Dahbi, David Violleau, Fouad Ghamouss, Johan Jacquemin, François Tran-Van, Daniel Lemordant, and Mérièm Anouti*

Laboratoire PCMB (EA 4244), Université François Rabelais, Parc de Grandmont 37200 Tours, France

Ⓢ Supporting Information

ABSTRACT: For a better understanding of the adsorption behavior of alkylcarbonate-based electrolytes on graphite electrodes and Celgard separator for Li-ion batteries applications, the interface parameters are determined by contact angle and surface tension measurements. The correlation between these parameters and chemical compositions made of alkyl carbonate with a varying nature of lithium salts (LiPF$_6$ and LiTFSI) and volume fractions of binary and ternary mixtures containing propylene carbonate (PC), ethylene carbonate (EC), and dimethyl carbonate (DMC) is investigated. From the obtained contact angle and surface tension (γ_L) values for each liquid, the dispersive and polar components of the surface tension (γ_L^d and γ_L^p) of the electrolyte and interfacial free energy between the solid and liquid (γ_{SL}) were then calculated using the Young's equation. The variation of contact angle (θ) and the surface tension, as well as the work of adhesion (W_A) of binary PC/DMC mixtures on PP, PE, and PET model surfaces were also measured and commented as function of volume fraction of PC in DMC. Finally, the Zisman's critical surface tension (γ_C) for studied surfaces was then obtained showing positives slopes of cos θ versus γ_L. This behavior is explained by a relative higher adsorption of alkylcarbonates to the hydrogenated supports or graphite. These results are decisive to understand the performance of electrolyte/electrode material/separator interfaces in lithium-ion battery devices.

1. INTRODUCTION

Advanced electrochemical systems with high performance are now required for energy storage and electric vehicle applications. For such system like lithium ion batteries, the development of a new electrolyte with stability and safety constitutes a considerable challenge. For these systems, the most common electrolytes used consist of a mixture of different alkylcarbonates with a lithium salt.[1−4] Although many contributions on thermodynamic properties of alkylcarbonates mixed with salts are described in the literature, little information is provided about interactions between the electrolyte and an interface like an electrode or a separator. This situation has restricted the application of new electrolytes to some extent, as thermodynamic data are generally the prerequisites for the process formulation and design, especially, the thermal stability, vapor pressure, and interfacial properties of each mixture.

The selection of salts to be dissolved in alkylcarbonates as solvents is decisive in providing highly conductive electrolytes. These salts are often chosen among salts of very strong acids or superacids such as LiClO$_4$, LiBF$_4$, LiAsF$_6$, LiPF$_6$, or CF$_3$SO$_3$Li.[5−7] Nevertheless, some of them are sometimes dangerous and unstable in contact with highly reactive lithium metal and have a limited stability toward oxidation which restricts the selection of these as cathode materials. As for anions of super acids such as AsF$_6^-$, BF$_4^-$, and PF$_6^-$, they are the result of an acid–base equilibrium with the corresponding Lewis acid, influenced by the electron-donating ability of the solvent and the polarizing nature of Li$^+$. Special attention has therefore been paid to new lithium salts meeting the previous requirements, that is, thermal and electrochemical stabilities.

Currently, the state-of-art electrolyte for a Li-ion battery is composed of lithium hexafluorophosphate (LiPF$_6$) salt dissolved in a mixture of cyclic carbonates like ethylene carbonate (EC) or propylene carbonate (PC) and linear esters such as dimethyl carbonate (DMC), diethyl carbonate (DEC). LiPF$_6$ has been used as the salt in Li-ion batteries for more than a decade because of its unique balance of properties such as good ionic conductivity and ability to passivate an aluminum current collector. However, LiPF$_6$ is thermally unstable and decomposes in LiF and PF$_5$ that can trigger detrimental reactions on the electrode surfaces.[8,9] In addition, LiPF$_6$ and PF$_5$ react with residual water to form HF.[6] Lithium imide salt is potentially a good alternative to LiPF$_6$ since it could both improve the chemical and thermal stability of the electrolyte. Particularly, the lithium bis(trifluoromethylsulfonyl)imide (LiTFSI) salt is well-known to be more stable and safer than the LiPF$_6$ salt.[10] However, LiTFSI salt is more corrosive than LiPF$_6$ toward an aluminum collector, and several studies were focused on this phenomenon.[11−14] We recently proposed a comparative study of performance for two binary systems, EC/DMC with LiPF$_6$ and LiTFSI salts. Results show the difference between their electrochemical performances.[15] To complete these results we present herein the investigation of their

interfacial properties on graphite electrodes and polymeric support monolayers PP, PE, and PET or the Celgard 2325 separator commonly used in Li-ion batteries.

2. EXPERIMENTAL SECTION

2.1. Reagents and Supports. Ethylene carbonate (EC) (>99%), dimethyl carbonate and (DMC) (>99%), lithium hexafluorophosphate (LiPF$_6$), lithium and bis-(trifluoromethylsulfonyl)imide, LiN(SO$_2$CF$_3$)$_2$, (LiTFSI) salts were obtained from Aldrich and used without further purification. Water content in each solvent used was measured by using a Metrohom Karl–Fisher titrator and was found to be lower than 20 ppm. Electrolyte solutions were prepared in a glovebox filled with argon, the water content of the freshly prepared electrolyte solutions was found to be close to 30 ppm. The graphite electrodes tested contained 95% graphite 2% acetylene carbon black and 3% PVDF HFP coated on a copper collector (thickness 200 μm). The graphite used is SLP30 type with a particle size of 31 μm and a BET surface of 7 m^2·g^{-1}. Celgard 2325 separators have pores size of (0.09 × 0.04) μm, thickness of 25 μm, and Gurley 23S.

2.2. Measurements. *Contact Angles.* The contact angles (CA) were measured according to the sessile drop method using a G-11 goniometer (Krüss, Germany), at room temperature (25 ± 2 °C). A single drop of the test liquid (drop volume ca. 3−5 μL) was placed on the support via a microlitre syringe, which was first rinsed with the tested liquid. Dynamic contact angles were measured on a picture of the drop obtained using acquisition of measurements software. For each support, the contact angle was determined six times at different positions on the material, and the average values are reported. The lowest and the highest values were disregarded, and the remaining values were used to calculate the arithmetic mean and the standard deviation. For each sample, the standard deviation for CA measurements was less than 3°, which involves a standard deviation for surface free energy calculations of 6%.

Liquid Surface Free Energy (SFE). The liquid surface free energy (SFE) has been measured from a Lauda tensiometer (Germany) using the ring method. The measurements were done in such a way that the vertically hung ring was dipped into the liquid to measure its surface tension, which was then pulled out. The maximum force needed to pull the ring through the interface was then expressed as the surface tension, γ_L (mN·m^{-1}). This apparatus was first calibrated with pure water to ensure accuracy and reliability of reported data. The experimental surface free energy of pure water was obtained to be close to 72.5 mJ·m^{-2}, which is in good agreement with reported literature values.[16]

3. RESULTS AND DISCUSSION

3.1. Surface-Tension Components of Binary and Ternary Systems. Characterizations and predictions of wetting phenomenon using contact angle (CA) measurements through the sessile drop method and surface free energy (SFE) calculations are powerful analysis tools widely used for many interfacial applications like lithium ion batteries or super-capacitors because of the interfacial electrode/separator problems of these systems.[17] The thermodynamic overview of the sessile drop method was first described by Young and reported by Spelt et al.,[18] from which different relations between the surface free energies of a liquid, a solid and a gas,

and the CA formed at the interface of these three phases were addressed. The surface free energy of a liquid is easily obtained by using surface tension measurements, which is not often the case with solids.

For applications involving heterogeneous systems and transport of electrolytes into interfaces such as fibrous membranes, or porous environments, interfacial properties such as wettability and adhesion of electrolyte are critical. This subject, however, has received so far only limited attention. In this study, interfacial properties of six systems: neat solvents (EC/DMC; EC/PC/3DMC) and their mixture with 1 M LiPF$_6$ or 1 M LiTFSI have been investigated for smooth surfaces (PE, PP, and PET). These surfaces are chosen because Celgard separators used in lithium ion battery or supercapacitors are composed from these materials.[19] First, we report herein contact angles (θ) for studied systems on these different surfaces; second, we describe in this work the surface tension (γ_L) of the six studied electrolytes. On the basis of these measurements, effects of surface nature and added salt on electrolyte wettability have been investigated.

The substrates (PP, PE, PET, graphite electrodes, and Celgard 2325 separator) were carefully cleaned in a detergent solution, rinsed with distilled and deionized water, dried with nitrogen, and finally dried for 2 h inside a vacuum oven at room temperature. The surface tension and the contact angle measurements were carried out by the pendant and the sessile drop methods. The contact angle measurements were made at room temperature as a function of time until stable values were achieved as shown for graphite and Celgard 2325 as an example in the snapshots of Figure 1.
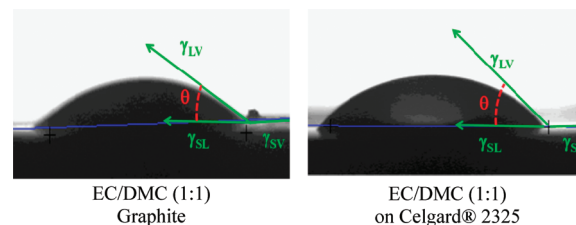

Figure 1. Contact angle snapshots for solvents on graphite and Celgard separator.

Prior to the discussion of the results, it should be stated that the free surface energy (FSE), γ_S, of the solid surfaces cannot be easily obtained directly from the experiments. In other words, γ_S can be obtained indirectly, for example, from the wettability data using different approaches described in the literature. Perhaps, the most frequently used are the methods of the surface-energy components.[20]

In this method, the total free surface energy γ_S is obtained as a sum of its dispersive (γ_S^d) and polar (γ_S^p) components:

$$\gamma_S = \gamma_S^d + \gamma_S^p \tag{1}$$

$$\gamma_L = \gamma_L^d + \gamma_L^p \tag{2}$$

$$\gamma_L(1 + \cos(\theta)) = 2(\sqrt{\gamma_S^d \gamma_L^d} + \sqrt{\gamma_S^p \gamma_L^p}) \tag{3}$$

The superscripts d and p are related to the dispersive and polar components of the SFE, respectively. To use eq 3, the dispersive and polar components of the surface used γ_S^d and γ_S^p must be known. For that a set of two liquids, one dispersive liquid, diiodomethane ($\gamma_S^p = 1$), and one polar liquid, formamide

($\gamma_S^d = 0$), is employed. Contact angle measurements (θ), SFE (γ_S), and its dispersive (γ_S^d) and polar (γ_S^p) component values for formamide (F) and diodomethane (D) on graphite electrodes and Celgard 2325 separator measured into this work are reported in Table S1 of the Supporting Information, the values reported in the cases of PE, PP, and PET were taken from our previous work.[19]

Equation 2 can be used to determine the dispersive and polar components of the surface tension (γ_L^d and γ_L^p) of the electrolyte. Calculation of the interfacial free energy between the solid and liquid (γ_{SL}) phase was performed using the Young's equation:

$$\gamma_L \cos(\theta) = \gamma_S - \gamma_{SL} \qquad (4)$$

The results are shown in Tables 1 and 2 for involved binary and ternary systems, respectively.

Table 1. Surface Tension γ_L (mN·m^{-1}), Free Surface Energy of the Monolayers γ_{SL} (mN·m^{-1}), Dispersive and Polar Components of the Surface Tension of the Binary System Fluid (γ_L^d), and Polar (γ_L^p) (mN·m^{-1}) and Zisman's Critical Surface Tension (γ_C) (mN·m^{-1}) of the Monolayer Components Derived from the Contact Angles

binary system		EC/ DMC	EC/DMC LiPF$_6$	EC/DMC LiTFSI
γ_L		32.7	30.3	30.0
PE, $\gamma_C = 40.5$	θ (deg)	43.0	49.8	50.5
	γ_L^d	17.4	13.1	12.6
	γ_L^p	15.3	17.2	17.4
	γ_{SL}	9.0	13.3	13.8
PP, $\gamma_C = 38.8$	θ (deg)	45.3	54.0	55.0
	γ_L^d	15.9	10.7	10.2
	γ_L^p	16.9	19.6	19.8
	γ_{SL}	12.7	17.9	18.5
PET, $\gamma_C = 38.4$	θ (deg)	46.5	56.1	57.5
	γ_L^d	7.7	4.1	3.8
	γ_L^p	25.1	26.2	26.2
	γ_{SL}	16.6	22.2	23.0
Celgard 2325, $\gamma_C = 39.8$	θ (deg)	44.5	52.0	53.0
	γ_L^d	20.4	14.9	14.2
	γ_L^p	12.3	15.4	15.8
	γ_{SL}	10.1	14.7	15.4
graphite, $\gamma_C = 40.4$	θ (deg)	25.1	29.0	29.0
	γ_L^d	7.5	5.4	5.4
	γ_L^p	25.3	24.9	24.6
	γ_{SL}	20.6	23.7	24.0

From values reported in Table 1, it can be noted that in the case of the (EC/DMC) binary system, the addition of salt increases γ_{SL} for all supports. Knowing that low values of γ_{SL} reflect the affinity between liquid and material, we can conclude that the salt decreases this affinity. The addition of PC in the electrolytes (Table 2) reduces the surface energy in the case of solvent mixtures without salts, as well as when salts are added for all materials. The effect of the addition of PC in both cases is significant, in that it involves a decrease of the energy γ_{SL}. This observation suggests that in the ternary mixture, a preferred interaction is between the PC and materials, promoting its presence at the interface. To understand the effect of PC on the lowering of this energy, we have studied the evolution of the interfacial properties (γ_L, θ) in the whole composition range of PC/DMC.

Table 2. Surface Tension γ_L (mN·m^{-1}), Free Surface Energy of the Monolayers γ_{SL} (mN·m^{-1}), Dispersive and Polar Components of the Surface Tension of the Ternary System Fluid (γ_L^d), and Polar (γ_L^p) (mN·m^{-1}) and Zisman's Critical Surface Tension (γ_C) (mN·m^{-1}) of the Monolayer Components Derived from the Contact Angles

ternary system		EC/PC/ 3DMC	EC/PC/ 3DMC LiPF$_6$	EC/PC/3DMC LiTFSI
γ_L		32.0	33.2	33.5
PE, $\gamma_C = 40.5$	θ (deg)	45.0	42.0	41.0
	γ_L^d	16.7	19.5	20.4
	γ_L^p	15.3	13.7	13.1
	γ_{SL}	10.3	8.3	7.6
PP, $\gamma_C = 38.8$	θ (deg)	47.9	43.7	42.0
	γ_L^d	14.1	16.9	17.9
	γ_L^p	17.9	16.3	15.6
	γ_{SL}	14.3	11.7	10.8
PET, $\gamma_C = 38.4$	θ (deg)	49.8	45.0	43.0
	γ_L^d	6.4	8.4	9.2
	γ_L^p	25.6	24.8	24.3
	γ_{SL}	18.5	15.7	14.6
Celgard 2325, $\gamma_C = 39.8$	θ (deg)	47.1	43.0	42.0
	γ_L^d	18.5	21.5	22.4
	γ_L^p	13.5	11.6	11.1
	γ_{SL}	11.6	9.2	8.5
graphite, $\gamma_C = 40.4$	θ (deg)	26.0	24.0	23.9
	γ_L^d	6.8	7.9	8.2
	γ_L^p	25.2	25.2	25.3
	γ_{SL}	21.5	19.9	19.6

3.2. Effect of Composition in the PC/DMC Binary System on Wettability and Adhesion Energy.

Binary mixtures of PC/DMC were chosen for the experiment because these alkyl carbonates are liquids at $T = 25\,°C$ and their surface tensions γ_L are sufficiently different ($\gamma_L = 45$ mN·m^{-1} for PC, and $\gamma_L = 31.9$ mN·m^{-1} for DMC). The obtained values of the advancing contact angles (θ) and surface tension (γ_L) of PC/DMC binary mixtures as a function of volume fraction of PC are presented in Figure 2 and in Table S2 of the Supporting Information. It appears that both values increased when there was an increase in the volume fraction of PC with linear relationships between them, θ from 17.6 to 51.5° and γ_L from 31.9 to 45.0 mN·m^{-1}. Table S2 (see Supporting Information) presents also the free surface energy of the monolayers γ_{SL} (mN·m^{-1}) as well as the dispersive (γ_L^d) and polar components (γ_L^p) of the surface tension in the case of the PC/DMC binary system on different material supports. We can note from these results that the free surface energy of the monolayers γ_{SL} for pure PC is two times higher for PC compared to the DMC on PP and PE; this tendency is reversed with the PET monolayer. The changes in the support surface tension with the molar fraction of alkylcarbonates electrolytes and their mixtures is also reflected by the values of the work of adhesion W_A

$$W_A = \gamma_L + \gamma_S - \gamma_L(\cos\theta + 1) \qquad (5)$$

which can also be formulated as

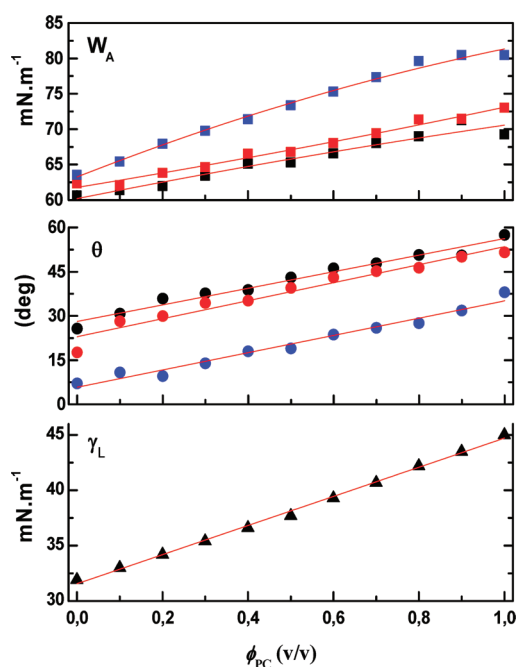$$\gamma_L \cos\theta = -\gamma_L + W_A \qquad (6)$$

Figure 2. Variation of the surface tension (γ_L), contact angle (θ), and adhesion energy (W_A) as a function of the volume fraction of PC in (DMC/PC) binary system, on PP (black), PE (red), and PET (blue) surfaces.

For all supports tested (PP, PE, and PET) with PC/DMC mixtures, a linear dependence occurs between the adhesion tension and the surface tension of each solution, with W_A values ranging from (80 to 60.6) mN·m^{-1} according to the supports and compositions of the binary system used.

3.3. Zisman's Critical Surface Tension. The critical surface tension is defined as the intercept of the horizontal line, $\cos \theta = 1$,[21] with the extrapolated straight-line plot of $\cos(\theta)$ against γ_L as shown in Figure 3. This intersection is the point where the contact angle is 0°. A hypothetical test liquid having this γ_L would just spread over the substrate. Zisman's critical surface tension (γ_C) for the surfaces studied in this work, were then obtained by using different extrapolations to the value of $\cos \theta = 1$ and are reported in Table 2.

A direct method to investigate relative adsorption at interfaces in wetting studies was developed by Lucassen-Reynders.[23] By combining the Young and Gibbs equations, it was shown that

$$\frac{d(\gamma_L \cos \theta)}{d\gamma_L} = \frac{\Gamma_S - \Gamma_{SL}}{\Gamma_L} \qquad (7)$$

where Γ_S, Γ_{SL}, and Γ_L represent the surface excess of the surfactants at the solid−air, solid−liquid, and liquid−air interfaces, respectively. Assuming that an excess of the surfactants represents a variation in free surface energy and $\Gamma_S \approx 0$, it is then possible to establish from eq 7 the ratio of Γ_{SL} to Γ_L by plotting $\cos \theta$ vs γ_L. It is interesting that in the case of all surfaces studied here, the relationships between $\cos \theta$ vs γ_L have positive slopes. According to the Lucassen-Reynders equation, eq 5,[22] these positive slopes indicate that material wetting is impaired ($\Gamma_S \neq 0$) by the addition of the binary or ternary mixture because of the "phobicity" of the alkylcarbonates and lithium salts containing Fluor atoms. On the other hand, these positive slopes of the curves indicate that the
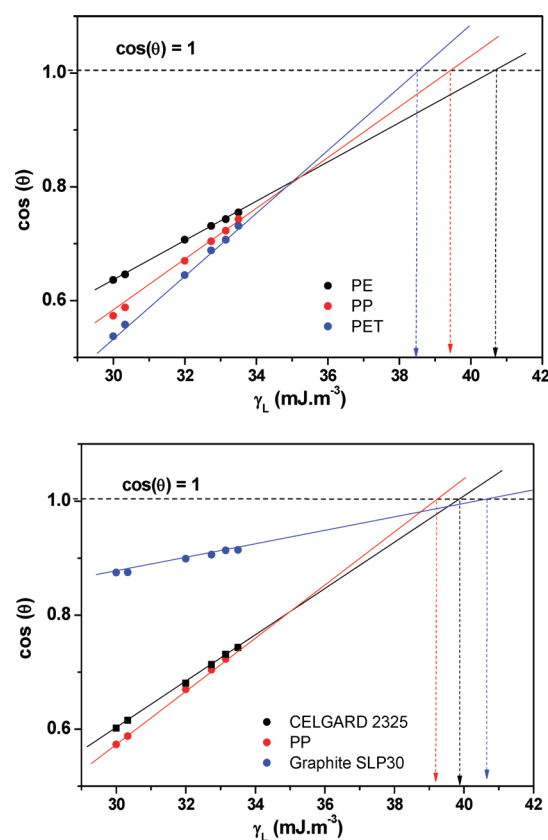

Figure 3. Zisman's plots ($\cos \theta$ vs γ_L) for EC/DMC, EC/PC/3DMC, EC/PC +LiPF$_6$ (1M), EC/DMC + LiTFSI (1M), EC/PC/3DMC +LiPF$_6$ (1M), EC/PC/3DMC + LiTFSI (1M) systems on (a) PE, PP, and PET surfaces; (b) graphite, PP, and Celgard 2325 materials.

surface excess concentration of electrolyte components at the material−air interface is higher than zero, and the surface excess concentration of solute at the material−electrolyte interface is $\Gamma_{SL} < 0$. The addition of PC changes notably the behavior of the electrolyte on the surface material especially in the case of LiTFSI-based electrolytes. We can claim from Figure 3 that the optimal surface tension γ_L for best wettability for graphite and Celgard 2325 is in the 40 to 41 mN·m^{-1} interval.

Fowkes[23] proposes that the surface tension in the solid−fluid interfacial tensions is the sum of several components, each due to a specific type of intermolecular force across an interface between two bulk phases, that is, London dispersion forces, hydrogen bonds, electron acceptor-electron donor forces, etc. The interface between two bulk phases therefore allows the evaluation of γ_S and γ_{SL} in conjunction with Young's equation. Otherwise the adsorption of a molecule for one component of the mixture at the solid/water interface leads to a layer or film formation on the solid surface, which affects its surface tension.[24,25] The presence of a high interaction between the alkylcarbonate and surface changes the contact angle in the solid−liquid drop−air system, which is linked to the measure of its wettability. There are also inconsistent opinions concerning the correlation between the critical surface tension of wetting of a given solid (γ_C) and its surface tension.[26,27] Some investigators suggest that the critical surface tension of wetting is a unique property of solids and is close to their surface tensions, but others state that it is possible to determine more than one γ_S value for a given solid depending on the type of the liquid used for contact angle measurements on this solid.[26−30]

5243

dx.doi.org/10.1021/ie203066x | *Ind. Eng. Chem. Res.* 2012, 51, 5240−5245

In the case of supports studied herein, the higher interactions between alkylcarbonates and hydrogen in hydrogenated polymer supports (PP, PE) or graphite electrodes confirm the evolution of γ_S with these supports. The addition of fluorinated-based lithium salts increases in fact for these interactions.

4. CONCLUSION

The surface tension and contact angles on polymeric model substrates namely PP, PE, and PET as well as Celgard separator and graphite electrodes for lithium-ion batteries technology were determined in this work. From these data, it was possible to infer about the polarity of the liquids from the dispersive and polar components of the surface tension (γ_L^d and γ_L^p) and by evaluation of γ_S and γ_{SL} in conjunction with Young's equation. For model supports tested (PP, PE, and PET) a linear dependence occurs between surface tension (γ_L), contact angle (θ), and adhesion energy (W_A) as a function of the volume fraction of PC in (DMC/PC) binary system with W_A values ranging from 80 to 60.6 mN·m^{-1}. Finally, Zisman's critical surface tension (γ_C) for the surfaces were then obtained showing positives slopes of cos θ vs γ_L. This behavior is explained by a relative higher adsorption of alkylcarbonates to hydrogenated supports or graphite materials which is linked to the measure of its wettability. These results are decisive to understand the performance of electrolyte/electrode material/separator interfaces in lithium ion batteries.

■ ASSOCIATED CONTENT

Ⓢ Supporting Information

Contact angles, surface tensions, and free surface energies values for formamide (F), diiodomethane (D), and for the PC/DMC binary system on graphite electrodes and Celgard 2325 separator are shown in Tables S1 an S2, respectively. This material is available free of charge via the Internet at http://pubs.acs.org.

■ AUTHOR INFORMATION

Corresponding Author
*Tel.: +33(0)247366951. Fax: +33(0)247367073. E-mail: meriem.anouti@univ-tours.fr.

Notes
The authors declare no competing financial interest.

■ ACKNOWLEDGMENTS

■ REFERENCES

(1) Buqa, H.; Würsig, A.; Goers, D.; Hardwick, L. J.; Holzapfel, M.; Novák, P.; Krumeich, F.; Spahr, M. E. Behaviour of highly crystalline graphites in lithium-ion cells with propylene carbonate containing electrolytes. *J. Power Sources* **2005**, *146*, 134.

(2) Buqa, H.; Würsig, A.; Vetter, J.; Spahr, M. E.; Krumeich, F.; Novák, P. SEI film formation on highly crystalline graphitic materials in lithium-ion batteries. *J. Power Sources* **2006**, *153*, 385.

(3) Lee, C. W.; Sun, Y.-K.; Prakash, J. A novel layered Li [Li$_{0.12}$Ni$_z$Mg$_{0.32}$−zMn$_{0.56}$]O$_2$ cathode material for lithium-ion batteries. *Electrochim. Acta* **2004**, *49*, 4425.

(4) Nakajima, T.; Dan, K.-I.; Koh, M.; Ino, T.; Shimizu, T. Effect of addition of fluoroethers to organic solvents for lithium ion secondary batteries. *J. Fluorine Chem.* **2001**, *111*, 167.

(5) Jung, C. Electrochemical absorption effect of BF$_4$ anion salt on SEI layer formation. *Solid State Ionics.* **2008**, *179*, 1717.

(6) Chen, Z.; Lu, W. Q.; Liu, J.; Amine, K. LiPF$_6$/LiBOB blend salt electrolyte for high-power lithium-ion batteries. *Electrochim. Acta* **2006**, *51*, 3322.

(7) Zhang, Z.; Chen, X.; Li, F.; Lai, Y.; Li, J.; Liu, P.; Wang, X. LiPF$_6$ and lithium oxalyldifluoroborate blend salts electrolyte for LiFePO$_4$ artificial graphite lithium-ion cells. *J. Power Sources* **2010**, *195*, 7397.

(8) Wang, H.; Yoshio, M.; Thapa, A. K.; Nakamura, H. From symmetric AC/AC to asymmetric AC/graphite, a progress in electrochemical capacitors. *J. Power Sources* **2007**, *169*, 375.

(9) Aurbach, D.; Talyosef, Y.; Markovsky, B.; Markevich, E.; Zinigrad, E.; Asraf, L.; Gnanaraj, S. J.; Kim, H.-J. Design of electrolyte solutions for Li and Li-ion batteries: A review. *Electrochim. Acta* **2004**, *50*, 247.

(10) Sylla, S.; Sanchez, J. Y.; Armand, M. Electrochemical study of linear and crosslinked POE-based polymer electrolytes. *Electrochim. Acta* **1992**, *37*, 1699.

(11) Han, H.-B.; Zhou, S.-S.; Zhang, D.-J.; Feng, S.-W.; Li, L.-F.; Liu, K.; Feng, W.-F.; Nie, J.; Li, H.; Huang, X.-J.; Armand, M.; Zhou, Z.-B. Lithium bis(fluorosulfonyl)imide (LiFSI) as conducting salt for nonaqueous liquid electrolytes for lithium-ion batteries: Physicochemical and electrochemical properties. *J. Power Sources* **2011**, *196*, 3623.

(12) Abouimrane, A.; Ding, J.; Davidson, I. Nanotextured gold coatings on carbon nanofiber scaffolds as ultrahigh surface-area electrodes. *J. Power Sources* **2009**, *189*, 693.

(13) Garcia, B.; Armand, M. Aluminium corrosion in room temperature molten salt. *J. Power Sources* **2004**, *132*, 206.

(14) Krause, J. L.; Lamanna, W.; Summerfield, J.; Engle, M.; Korba, G.; Loch, R.; Atanasoski, R. Corrosion of aluminum at high voltages in non-aqueous electrolytes containing perfluoroalkylsulfonyl imides; new lithium salts for lithium-ion cells. *J. Power Sources* **1997**, *68*, 320.

(15) Dahbi, M.; Ghamouss, F.; Tran-Van, F.; Lemordant, D.; Anouti, M. Comparative study of EC/DMC LiTFSI and LiPF$_6$ electrolytes for electrochemical storage. *J. Power Sources* **2011**, *196*, 9743.

(16) Henn, A. R. The surface tension of water calculated from a random network model. *Biophys. Chem.* **2003**, *105*, 533.

(17) Good, R. J. Contact angle, wetting, and adhesion: a critical review. *J. Adhes. Sci. Technol.* **1992**, 1269.

(18) Spelt, J. K.; Li, D. The equation of state approach to interfacial tensions. In *Applied Surface Thermodynamics*; Neumann, A. W., Spelt, J. K., Eds.; Marcel Dekker: New York, 1996; 239−292.

(19) Stefan, C. S.; Lemordant, D.; Montigny, B. C.; Violleau, D. Are ionic liquids based on pyrrolidinium imide able to wet separators and electrodes used for Li-ion batteries ? *J. Power Sources* **2009**, *189*, 1174.

(20) Van Oss, C. J. *Interfacial Forces in Aqueous Media*, 2nd ed.; Taylor & Francis: London, 2006.

(21) Zisman, W. A. Contact angle, wettability and adhesion. *Adv. Chem. Ser.* **1964**, *43*, 1.

(22) Lucassen-Reynders, F. H. Surface equation of state for ionized surfactants. *J. Phys. Chem.* **1966**, *70*, 1777.

(23) Fowkes, F. M. Attractive forces at interfaces. *Ind. Eng. Chem.* **1964**, *56*, 40.

(24) Rosen, J. M. *Surfactants and Interfacial Phenomena*; Wiley-Interscience: New York, 2004.

(25) Tabor, R. F.; Eastoe, J.; Dowding, P. J. A two-step model for surfactant adsorption at solid surfaces. *J. Colloid Interface Sci.* **2010**, *346*, 424.

(26) Valentine, T. M. On the use of critical energy techniques for the measurement of surface energies of ceramics: Part II. The temperature variant method. *Mater. Sci. Eng.* **1977**, *3*, 211.

(27) Szymczyk, K.; Jańczuk, B. Wettability of a polytetrafluoroethylene surface by an aqueous solution of two nonionic surfactant mixtures. *Langmuir* **2007**, *23*, 8740.

(28) Becher, P. Interaction parameter calculations from contact angle data. *J. Colloid Interface Sci.* **1977**, *3*, 429.

(29) Bernett, M. K.; Zisman, W. A. Relation of wettability by aqueous solutions to the surface constitution of low-energy solids. *J. Phys. Chem.* **1959**, *63*, 1241.

(30) Bargeman, D.; van Voorst Vader, F. Effect of surfactants on contact angles at nonpolar solids. *J. Colloid Interface Sci.* **1973**, *42*, 467.